PHYSICAL REVIEW C **78**, 031901(R) (2008)

Nuclear stopping and sideward-flow correlation from 0.35A to 200A GeV

Xiao-Feng Luo,* Ming Shao, Xin Dong, and Cheng Li
University of Science and Technology of China, Hefei, Anhui 230026, People's Republic of China
(Received 10 June 2008; published 10 September 2008)

The correlation between the nuclear stopping and the scale invariant nucleon sideward flow at energies ranging from those available at the GSI heavy ion synchrotron (SIS) to those at the CERN Super Proton Synchrotron (SPS) is studied within ultrarelativistic quantum molecular dynamics (UrQMD). The universal behavior of the two experimental observables for various colliding systems and scale impact parameters are found to be highly correlated with each other. As there is no phase transition mechanism involved in the UrQMD, the correlation may be broken down by the sudden change of the bulk properties of the nuclear matter, such as the formation of quark-gluon plasma (QGP), which can be employed as a QGP phase transition signal in high-energy heavy ion collisions. Furthermore, we also point out that the appearance of a breakdown of the correlation may be a powerful tool for searching for the critical point on the QCD phase diagram.

DOI: 10.1103/PhysRevC.78.031901 PACS number(s): 25.75.Ld, 24.10.Jv, 24.10.Lx, 25.70.Pq

In recent years, the main aim of studies of ultrarelativistic high-energy heavy ion collisions (HICs) performed at the CERN Super Proton Synchrotron (SPS) ($\sqrt{s_{\rm NN}} \sim 10A$ GeV) and the BNL Relativistic Heavy Ion Collider (RHIC)($\sqrt{s_{\rm NN}} \sim 200A$ GeV) has been to search for a new form of matter with partonic degrees of freedom, the so-called quark-gluon plasma (QGP) [1–4]. Although great effort has been made, no dramatic changes of experimental observables, such as jet quenching, elliptic flow, and strangeness enhancement, have been observed yet, and it is hard to make a solid conclusion for the occurrence of the QGP phase transition [5]. Recently, an energy scan program has been proposed for RHIC to perform HIC experiments with lower c.m. energy to search for the critical point [6–8], which is an endpoint of the first-order phase transition line on the QCD phase diagram. If the critical point exists, it should appear on the QGP transition boundary at higher baryon chemical potential and lower colliding energy [9,10]. To extract the QGP phase transition signal, a large number of possible experimental probes, such as particle ratio and collective flow, have been proposed. The time evolution of temperature and baryon chemical potential of the different colliding nuclei with various colliding energies would be mapping a much broader T-μ_B region on the QCD phase diagram than for a single nucleus. However, it is complicated to uniformly and systematically obtain an unambiguous experimental signal for the QGP phase transition and to also mark the location of the critical point on the QCD phase diagram; one of the possible choices is to obtain insight into the universal correlation pattern of two experimental observables for various colliding systems (system size and beam energy). Thus, the complication of colliding-system dependence in searching for phase transition signals can be reduced.

In this work, the correlation between the nuclear stopping and scale invariant nucleon sideward flow within the framework of the UrQMD model from energies available at the GSI heavy ion synchrotron (SIS) to SPS energies has been found for various scale impact parameters $0 < b_0 = b/b_{\rm max} < 1$, not just for global fixed impact parameters as in Ref. [11]. The scale invariant nucleon sideward flow is defined as $\tilde{F}(b_0) = \partial(\langle p^x_{\rm c.m.}/A\rangle/p^{\rm proj}_{\rm c.m.})/\partial(y_{\rm c.m.}/y^{\rm proj}_{\rm c.m.})\big|_{[-1,1]}$, first proposed in Ref. [12], the linear fitting slope of the normalized rapidity dependence of the normalized average in reaction plane transverse momentum with a fitting range of $-1 < y_{\rm c.m.}/y^{\rm proj}_{\rm c.m.} < 1$, where $\langle p^x_{\rm c.m.}/A\rangle$ is the average transverse momentum projected in the reaction plane per nucleon, $p^{\rm proj}_{\rm c.m.}$ is the projectile momentum in the center-of-mass system (c.m.s.), and $y_{\rm c.m.}$ and $y^{\rm proj}_{\rm c.m.}$ are the nucleon rapidity and projectile rapidity in the c.m.s., respectively. The nuclear stopping ratio R as a measurement of degree of stopping of colliding nuclei at scale impact parameter b_0, suggested in Refs. [13,14], is expressed as $R(b_0) = \frac{2}{\pi}\sum_i |p_{ti}|/\sum_i |p_{zi}|$, where p_{ti} and p_{zi} are transverse and longitudinal momenta of the ith outgoing particle in the c.m.s., respectively. A colliding-system-dependent variable $\rho_{\rm mb}$ is also introduced as a normalization factor for later calculations. It is defined as $\rho_{\rm mb}(A, E_{\rm lab}) = {\rm MB}(0) \times u^{\rm proj}_{\rm c.m.}/A^{4/3}$, where the MB(0) stands for the meson-to-baryon ratio for central collision ($b_0 = 0$), $u^{\rm proj}_{\rm c.m.} = \beta^{\rm proj}_{\rm c.m.}\gamma^{\rm proj}_{\rm c.m.}$ is the spatial component of four-velocity of the projectile in the c.m.s., and A is the mass number of a nucleus in the symmetric colliding system. The overlapping volume of two colliding nuclei and the nuclear passing time for central collisions, respectively, satisfy $V \propto A$, and $t_{\rm pass} = r/u^{\rm proj}_{\rm c.m.} \propto A^{1/3}/u^{\rm proj}_{\rm c.m.}$, where r is the radius of nuclei. Thus, we have $\rho_{\rm mb} \propto {\rm MB}(0)/(V\, t_{\rm pass})$, standing for the meson-to-baryon ratio per unit volume per passing time in the central collisions, which is used to characterize the strength of particle production at early stage [15].

The UrQMD model [16] used here is a type of numerical transport model, which is based on the quark, diquark, string, and hadronic degrees of freedom. It includes 50 different baryon species (nucleon, hyperon, and their resonances up to 2.11 GeV) and 25 different meson species. Two types of equation of state, the hard EOS with incompressibility $K = 380$ MeV (only for beam energy up to 4A GeV) and the

*Contact author: science@mail.ustc.edu.cn

cascade EOS, are contained in the UrQMD model. The model has successfully been applied to reproduce the experimental results from SIS to SPS energies [17].

A group of symmetric colliding nuclei with five pairs, ^{197}Au + ^{197}Au, ^{129}Xe + ^{129}Xe, ^{96}Ru + ^{96}Ru, ^{58}Ni + ^{58}Ni, and ^{40}Ca + ^{40}Ca, are combined with 30 and 12 incident kinetic energies as follows. The first combination includes a total of $150 = 5 \times 30$ colliding systems with 30 beam energies per nucleon from 0.35 to 200 GeV (0.35, 0.5, 0.66, 0.83, 1.0, 1.5, 2.0, 3.0, 4.0, 5.3, 6.6, 8.0, 10.0, 10.93, 11.9, 12.9, 13.93, 15, 16.9, 17.92, 18.95, 20, 24.22, 36.0, 55.0, 76.92, 102.33, 131.33, 163.36, 200.0) for each pair of the colliding nuclei. The second one includes a total of $60 = 5 \times 12$ colliding systems with 12 beam energies per nucleon from 0.35 to 3.9 GeV (0.35, 0.5, 0.66, 0.83, 1.0, 1.5, 2.0, 2.35, 2.7, 3.1, 3.5, 3.9). They are researched with the cascade and hard EOSs of UrQMD, respectively.

Figure 1 shows the beam energy and system-size dependence of the central ($b_0 = 0$) nuclear stopping ratio $R(0)$ and the predefined variable $\rho_{\rm mb}$ as well as the semicentral ($0.3 < b_0 < 0.4$) scale invariant nucleon sideward flow $\tilde{F}(b_0)$ with the cascade EOS. In the left panels of Fig. 1, the $R(0)$ and $\tilde{F}(b_0)$ both decrease monotonously with the beam energy per nucleon from 0.35 to 200 GeV for three pairs of symmetric colliding nuclei, Au + Au, Ru + Ru, and Ca + Ca; and a larger nuclear stopping ratio is observed for heavier colliding nuclei than for the lighter one for a fixed beam energy. More detailed information on the system-size dependence of $R(0)$ and $\tilde{F}(b_0)$ is illustrated in the right panels of Fig. 1. Both $R(0)$ and $\tilde{F}(b_0)$ increase monotonously with mass number A, which is proportional to the size of the colliding system. The defined variable $\rho_{\rm mb}$, increasing with beam energy and decreasing with system size, is also shown in the lower panel of Fig. 1.

With the cascade EOS in UrQMD, the observables $R(0)$, $\rho_{\rm mb}$, and $\tilde{F}(b_0)$, with nonzero b_0 satisfying $0 < b_0 < 0.8$ and with an interval of 0.1, are calculated for the mentioned 150 colliding systems with beam energy per nucleon from 0.35

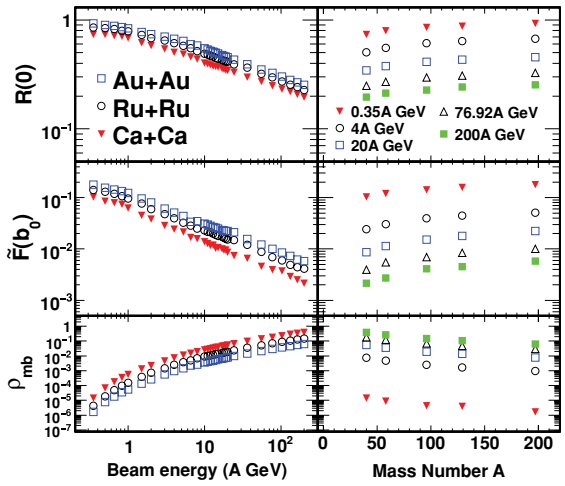

FIG. 1. (Color online) Left panels: excitation function of the central nuclear stopping ratio, the variable $\rho_{\rm mb}$, and the semicentral ($0.3 < b_0 < 0.4$) scale invariant nucleon sideward flow. Right panels: system-size dependence of the three experimental observables.

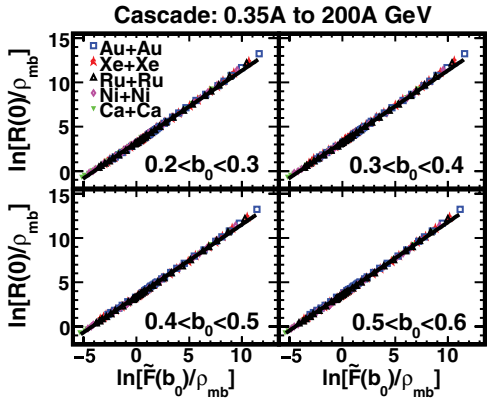

FIG. 2. (Color online) Correlation between the central nuclear stopping ratio and scale invariant nucleon sideward flow, with b_0 varying from 0.2 to 0.6 and an interval of 0.1, calculated for the mentioned 150 colliding systems within the cascade EOS. The solid line in each panel is the linear fit of the corresponding correlation.

to 200 GeV. After the logarithmic operations are performed on both normalized nuclear stopping $R(0)/\rho_{\rm mb}$ and normalized scale invariant nucleon sideward flow $\tilde{F}(b_0)/\rho_{\rm mb}$, the resulting two variables, $\ln[R(0)/\rho_{\rm mb}]$ and $\ln[\tilde{F}(b_0)/\rho_{\rm mb}]$, show strong universal correlation for various colliding systems with a given b_0 bin. For illustration, the correlation with the b_0 from 0.2 to 0.6 and the corresponding linear fit line are shown in Fig. 2. For the hard EOS case, the results of the mentioned 60 colliding systems with beam energy per nucleon from 0.35 to 3.9 GeV are shown in Fig. 3. The superposed solid line shown in Figs. 2 and 3 are the results of the linear fit for the corresponding correlation.

By the linear fit of the correlation in Figs. 2 and 3, the analytic relation between the two variables $R(0)$ and $\tilde{F}(b_0)$ can be expressed as

$$\ln\left[\frac{R(0)}{\rho_{\rm mb}}\right] = L \times \ln\left[\frac{\tilde{F}(b_0)}{\rho_{\rm mb}}\right] + m, \qquad (1)$$

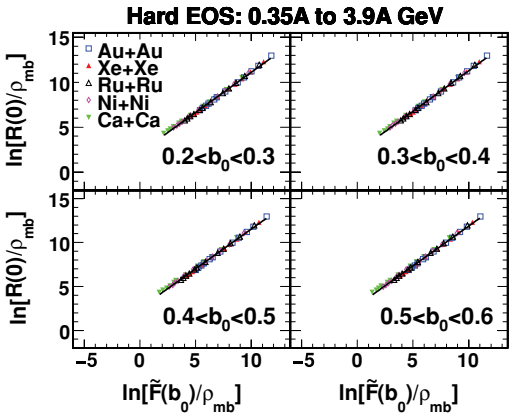

FIG. 3. (Color online) Correlation between the central nuclear stopping ratio and scale invariant nucleon sideward flow, with b_0 varying from 0.2 to 0.6 and an interval of 0.1, are calculated for the mentioned 60 colliding systems within the hard EOS. The solid line in each panel is the linear fit of the corresponding correlation.

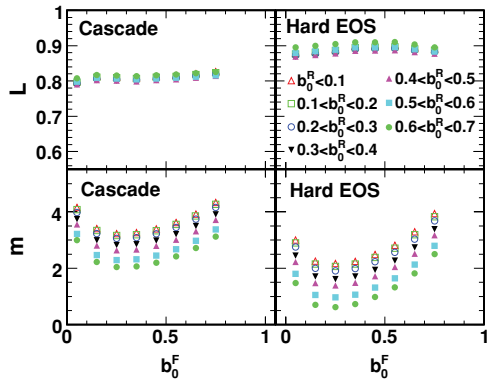

FIG. 4. (Color online) Dependence of fitting parameters slope L and intercept m on the scale impact parameters b_0^F and b_0^R for the cascade and hard nuclear EOSs.

where the two fitting parameters L and m are introduced to represent the slope and intercept, respectively. Generally speaking, there is nothing particular for any of the two variables R and $\tilde{F}$, and they are of equal importance. Actually, it is found that not only the central stopping ratio, but also the noncentral nuclear stopping ratio is correlated with the scale invariant nucleon flow $\tilde{F}(b_0)$, which means for two independent scale impact parameters b_0^R and b_0^F, the relation between the corresponding $R(b_0^R)$ and $\tilde{F}(b_0^F)$ can be expressed as

$$\ln\left[\frac{R(b_0^R)}{\rho_{\rm mb}}\right] = L \times \ln\left[\frac{\tilde{F}(b_0^F)}{\rho_{\rm mb}}\right] + m. \tag{2}$$

The fitting parameters L and m, depending on both b_0^F and b_0^R for the cascade and hard nuclear EOS cases, are illustrated in Fig. 4. In the two upper panels of Fig. 4, L shows almost no dependence on b_0^F and b_0^R, and it is larger for the hard EOS than for the cascade one. Thus, L can be regarded as a constant parameter for characterizing the nuclear EOS. In contrast, m is strongly affected by b_0^F, b_0^R and also by the different nuclear EOS, as seen in the lower panels of Fig. 4. The two parameters are both colliding-system independent, as they both are universal fitting parameters for various colliding systems. The parameter $m = m(b_0^F, b_0^R)$ is only a function of b_0^F and b_0^R, and the so-called correlation function $C(b_0^F, b_0^R) = e^{-m(b_0^F, b_0^R)}$ is defined to describe the correlation strength between the nuclear stopping ratio $R(b_0^R)$ and scale invariant nucleon sideward flow $\tilde{F}(b_0^F)$. Two new variables $R^*(b_0^R) = R(b_0^R)/\rho_{\rm mb}$ and $\tilde{F}^*(b_0^F) = \tilde{F}(b_0^F)/\rho_{\rm mb}$ are defined for simplification of Eq. (2). Then, it can be rewritten as

$$\tilde{F}^*(b_0^F) = \left(R^*(b_0^R) C(b_0^F, b_0^R)\right)^{\frac{1}{L}}, \tag{3}$$

where the correlation function, $0 < C(b_0^F, b_0^R) < 1$, is only related to b_0^F and b_0^R for a given nuclear EOS.

The colliding-system as well as scale-impact-parameter dependence of a single experimental observable is further investigated for any specific colliding system. From Eq. (3), for any given b_0^R and b_0^F, the two correlative observables are, respectively, calculated with two different scale impact parameters, (b_0^{F1}, b_0^{F2}) and (b_0^{R1}, b_0^{R2}), so then we have

$$\frac{\tilde{F}(b_0^{F1})}{\tilde{F}(b_0^{F2})} = \frac{e^{m(b_0^{F2}, b_0^R)/L}}{e^{m(b_0^{F1}, b_0^R)/L}}, \quad \frac{R(b_0^{R1})}{R(b_0^{R2})} = \frac{e^{-m(b_0^F, b_0^{R2})}}{e^{-m(b_0^F, b_0^{R1})}}. \tag{4}$$

The terms on the right side of the two equations in Eq. (4) are colliding-system independent, and the two equations are satisfied for any fixed b_0^R and b_0^F, respectively, which indicates that the variables of the two observables $\tilde{F}(b_0^F)$ and $R(b_0^R)$ can be separated into a colliding-system-dependent term multiplied by a scale-impact-parameter-dependent term, that is,

$$R(A, E_{\rm lab}, b_0^R) = \xi^R(A, E_{\rm lab}) \times \eta^R(b_0^R), \tag{5}$$

$$\tilde{F}(A, E_{\rm lab}, b_0^F) = \xi^F(A, E_{\rm lab}) \times \eta^F(b_0^F). \tag{6}$$

With the variable separable property, which is nontrivial and not common for all the experimental observables, the excitation properties of the correlative observables for any scale impact parameter are the same. To better understand the fitting parameters L and m, as well as the normalization factor $\rho_{\rm mb}$, Eqs. (5) and (6) are introduced into Eq. (2), then we obtain

$$\ln\left[\frac{\xi^R(A, E_{\rm lab})}{\rho_{\rm mb}}\right] = L \times \ln\left[\frac{\xi^F(A, E_{\rm lab})}{\rho_{\rm mb}}\right] + m(b_0^F, b_0^R) + L \times \ln\left[\eta^F(b_0^F)\right] - \ln\left[\eta^R(b_0^R)\right]. \tag{7}$$

As for various colliding systems $(A, E_{\rm lab})$ and scale impact parameters (b_0^F, b_0^R), for which Eq. (7) is always satisfied, we have

$$\ln\left[\frac{\xi^R(A, E_{\rm lab})}{\rho_{\rm mb}}\right] = L \times \ln\left[\frac{\xi^F(A, E_{\rm lab})}{\rho_{\rm mb}}\right], \tag{8}$$

$$m(b_0^F, b_0^R) = \ln\left[\eta^R(b_0^R)\right] - L \times \ln\left[\eta^F(b_0^F)\right]. \tag{9}$$

Equation (8) demonstrates that the colliding-system-dependent terms of the two correlative observables have been connected by introducing a proper normalization factor $\rho_{\rm mb}$, which is also colliding-system dependent and may be not unique for the present correlation or even not necessary for other correlative analyses. In Eq. (8), the universal fitting parameter L is uniquely determined by the colliding-system-dependent properties of the two observables, that is the reason the L is not related to the b_0^F and b_0^R for a given nuclear EOS (see Fig. 4). Thus, it is supposed to be a constant characteristic parameter for characterizing the nuclear intrinsic properties. The variable separable properties of the two correlative observables in Eqs. (5) and (6), and the analytic relation between colliding-system-dependent terms in Eq. (8) are the origin of the correlation presented by Eq. (2). As a consequence of the correlation for various scale impact parameters, the intercept parameter m can be expressed as Eq. (9), which is the combination of the scale-impact-parameter-dependent terms of the two correlative observables and without the cross terms. Derived from Eqs. (5), (6), and (9), the differential of

the parameter $m(b_0^F, b_0^R)$ can be written as

$$\frac{\partial m}{\partial b_0^R} = \frac{\partial \ln\left[\eta^R\left(b_0^R\right)\right]}{\partial b_0^R} = \frac{\partial \ln\left[R\left(A, E_{\rm lab}, b_0^R\right)\right]}{\partial b_0^R}, \quad (10)$$

$$-\frac{1}{L}\frac{\partial m}{\partial b_0^F} = \frac{\partial \ln\left[\eta^F\left(b_0^F\right)\right]}{\partial b_0^F} = \frac{\partial \ln\left[\tilde{F}\left(A, E_{\rm lab}, b_0^F\right)\right]}{\partial b_0^F}. \quad (11)$$

The differential of $m(b_0^F, b_0^R)$ in Eqs. (10) and (11) are only related to b_0^R and b_0^F, respectively (see Fig. 4), and uniquely determined by the corresponding experimental observable. The colliding-system-dependent properties of the differential of experimental observables in Eqs. (10) and (11) can be used to validate whether the observables are variable separable or not, which is a necessary and not sufficient condition for the present correlation. Because Eq. (2) is the fitting equation only for the two correlative observables, and not all the colliding systems exactly satisfy Eq. (2), the differential of m may be weakly dependent on the specific colliding system.

We have performed a correlative analysis between the nuclear stopping and scale invariant nucleon sideward flow for various colliding systems and scale impact parameters. The complication of the colliding-system dependence of a single observable can be separated from the scale-impact-parameter dependence and has been reduced to two universal fitting parameters L and m, which can be used to determine the nuclear EOS or other intrinsic properties. The essential of the universal correlation behavior between nuclear stopping and scale invariant nucleon sideward flow from SIS to SPS energies may result from the pressure of the matter in HICs, which is dominated by the nuclear EOS, in-medium NN cross section, etc., and intimately connected to the nuclear stopping and nucleon sideward flow [15,18–22]. The strong correlation may indicate that the pressure produced in HICs may be also with the variable separable property as in Eqs. (8) and (9), and it may be broken down by the sudden change of the nuclear bulk properties, such as phase transition. The phase transition mechanism is not explicitly involved in the UrQMD model, and it is also found in Ref. [23] that the collapse of the excitation function of the sideward flow and elliptic flow can be used to probe the first-order QGP phase transition. Thus, for qualitative analysis, it is predicted that the universal correlation may be broken down at different sets of beam energies for various colliding nuclei, which could serve as signals for the first-order QGP phase transition. Furthermore, if the universal correlation pattern is restored at much higher energies, where the crossover from hadronic phase to partonic phase would happen, the location of the critical point can be unitedly restricted by the mapping of different colliding nuclei with the corresponding lower limit of the restoration energies on the QCD phase diagram. The real experimental data as well as the theoretical calculation are expected to be compared with the UrQMD simulation results, and the detailed correlation mechanism of the two experimental observables should be further studied.

We thank Hong-Fang Chen, Zi-Ping Zhang, and Hu-Shan Xu for their helpful discussions. This work is supported by the National Natural Science Foundation of China (10775131, 10675111) and the CAS/SAFEA International Partnership Program for Creative Research Teams under Grant No. CXTD-J2005-1.

[1] C. Lourenco *et al.*, Nucl. Phys. **A698**, 13 (2002).
[2] N. Xu *et al.*, Nucl. Phys. **A751**, 109 (2005).
[3] J. Adams *et al.*, Nucl. Phys. **A757**, 102 (2005).
[4] K. Adcox *et al.*, Nucl. Phys. **A757**, 184 (2005).
[5] P. Jacobs and X. N. Wang, Prog. Part. Nucl. Phys. **54**, 433 (2005).
[6] P. Sorensen, arXiv:nucl-ex/0701028.
[7] ROYA. Lacey *et al.*, Phys. Rev. Lett. **98**, 092301 (2007).
[8] GSF Stephans, J. Phys. G: Nucl. Part. Phys. **35**, 044050 (2008).
[9] F. Karsch, arxiv:hep-lat/0601013v1.
[10] Z. Fodor and S. D. Katz, J. High Energy Phys. 03 (2002) 014.
[11] W. Reisdorf *et al.*, Phys. Rev. Lett. **92**, 232301 (2004).
[12] A. Bonasera and L. P. Csernai, Phys. Rev. Lett. **59**, 630 (1987).
[13] H. Ströbele *et al.*, Phys. Rev. C **27**, 1349 (1983).
[14] Xiao-Feng Luo *et al.*, Phys. Rev. C **76**, 044902 (2007).
[15] M. Bleicher and J. Aichelin, Phys. Lett. **B612**, 201 (2005).
[16] S. A. Bass *et al.*, arxiv:nucl-th/9803035.
[17] L. A. Winckelmann *et al.*, arxiv:nucl-th/9610033.
[18] Y. Zhang, Z. Li, and P. Danielewicz, Phys. Rev. C **75**, 034615 (2007).
[19] M. Isse, A. Ohnishi, N. Otuka, P. K. Sahu, and Y. Nara, Phys. Rev. C **72**, 064908 (2005).
[20] M. Bleicher *et al.*, Phys. Lett. **B447**, 227 (1999).
[21] V. N. Russkikh and Y. B. Ivanov, Phys. Rev. C **74**, 034904 (2006).
[22] H. Liu *et al.* (E895 Collaboration), Phys. Rev. Lett. **84**, 5488 (2004).
[23] Horst Stöcker, arXiv:0710.5089v1.